Research on Lane-Marking Line Based Camera Calibration

Kunfeng Wang, Hua Huang, Yuantao Li, and Fei-Yue Wang, *Fellow, IEEE*

***Abstract*— In this paper, we present a novel camera calibration method which requires only a few easy attainable lane markings in traffic scenes. All we need to know beforehand are a pair of parallel lane markings with known lane width and either the camera height or the length of a land marking parallel to the road. If the camera height is known a-prior, a set of camera parameters such as the focal length, the tilt angle, and the pan angle can be recovered; if the length of a land marking parallel to the road is known a-prior, not only the above camera parameters, but the camera height can also be recovered. We show experimentally that the proposed method is capable of achieving accurate results in most traffic monitoring applications, including inverse perspective transformation and even 3-D estimation of vehicle dimensions.**

I. Introduction

IN RECENT years, using cameras to estimate traffic conditions has greatly promoted the development of intelligent transportation systems. For a vision-based traffic monitoring system (VTMS), its basic function is to automatically extract real-time traffic parameters, including vehicle class, flow rate, occupancy, average velocity, and so on [1]-[4]. Although pursuing different goals, it is generally believed that VTMS is much more flexible and versatile if the camera is properly calibrated. The accuracy of vehicle speed estimation, for instance, depends heavily on the accuracy of camera calibration as well as tracking algorithms.

Camera calibration is an important issue which has received a considerable amount of attention in the literature. Accurate camera calibration requires the use of especially designed patterns to be placed in the field of view of the camera. However, in a traffic scene, this is usually not practical since one would need a very large calibration pattern left alone on the road [5]. Traditionally, researchers used low-level geometric features such as marked points and lines with little or hardly any geometric constraints in traffic scenes to recover camera parameters [1], [5]-[7]. Although theoretically sound, these methods potentially suffer from a serious problem. They require a large number of feature measurements to achieve robustness with complex computation. In practice, camera parameters, however, are subject to random and sometimes significant disturbances due to motion, thermal effects, environmental variation, or other unpredictable factors, and thus, cameras must be repeatedly calibrated and it becomes a time-consuming labor to localize a large set of features at each time [5], [8]. Therefore, an efficient camera calibration method that requires less preparation in setup and less computation in processing would be expected.

In this paper we present a method which requires a small set of easy attainable lane markings to calibrate traffic scenes. The *a prior* parameter set is comprised of two parallel lane-marking lines with known lane width and either the camera height or the length of a land marking parallel to the road. Lane-marking lines in the image are manually marked at this time; however, dynamic calibration can be achieved by integrating the automatic lane-marking recognition algorithm into the proposed method [3], [9], [10].

The remainder of this paper is organized as follows. Section II models the camera and roadway geometry and presents the equations of the world to image mapping. Section III addresses the recovery of camera parameters, including the focal length, the tilt angle, and the pan angle, given two parallel lane markings with known lane width as well as the camera height or the length of a land marking parallel to the road. Experimental results are presented in Section IV, followed by a conclusion in Section V.

II. Camera Model for Traffic Scenes

The task of camera calibration is to recover the intrinsic and extrinsic camera parameters. The intrinsic camera parameters involve the internal camera geometric and optical characteristics, including the focal length, the image center, the skew angle, and the aspect ratio. For reducing calibration complexity and enhancing its efficiency, we make a natural assumption that the intrinsic camera parameters, except for the focal length, are fixed and have been calibrated in the laboratory. The extrinsic camera parameters relate the camera's coordinated system to a fixed world coordinate system and specify its position and orientation in space. In this study we assume that the road is planar and there is a straight section of road in the scene.

The camera and roadway geometry similar to that used in [3] and [9] is depicted in Fig. 1. Three coordinate systems are utilized here: the world coordinate system $O-XYZ$, the

Manuscript received June 11, 2007. This work was supported in part by the MOST Grant 2006CB705500, NNSFC Grants 60334020, 60621001, CAS Grant 2F05N01, 2006 CAS Presidential Special Scholarship Grant, and SDAS Research Grant 2005006.

Kunfeng Wang and Yuantao Li are with the Key Laboratory of Complex Systems and Intelligence Science, Institute of Automation, Chinese Academy of Sciences, Beijing 100080, China (e-mail: kunfengwang@gmail.com; yuantao.li@ia.ac.cn).

Hua Huang is with the School of Electronic and Information Engineering, Xi'an Jiaotong University, Xi'an 710049, China, and also with the Key Laboratory of Complex Systems and Intelligence Science, Institute of Automation, Chinese Academy of Sciences, Beijing 100080, China (e-mail: xjhuanghua@sina.com).

Fei-Yue Wang is with the Key Laboratory of Complex Systems and Intelligence Science, Institute of Automation, Chinese Academy of Sciences, Beijing 10080, China, and also with the Department of Systems and Industrial Engineering, University of Arizona, Tucson, AZ 85719, USA (e-mail: feiyue@sie.arizona.edu).

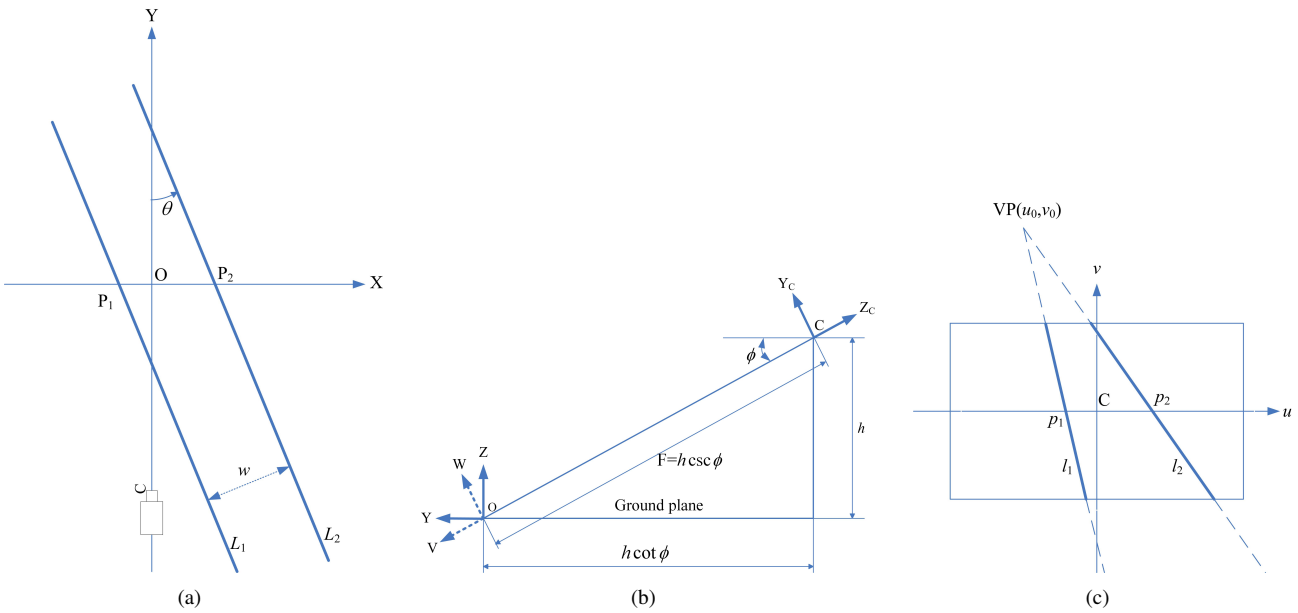

Fig. 1. Coordinate systems used to calibrate the camera overlooking a traffic scene: (a) Top view of the world coordinate system; (b) Side view of camera and road geometry with the coordinate systems used in the calibration; (c) Road geometry in the image showing the vanishing point for lines parallel to the road.

camera's coordinate system $C - X_C Y_C Z_C$, and the camera-shift coordinate system $O - UVW$. Fig. 1(a) depicts the bird view of road geometry with relevant X and Y axes. L_1 and L_2 are two parallel lane-marking lines and point C is the projection of the optical center of camera onto the road surface. The pan angle θ is the angle between Y axis and the lane markings, and w is the perpendicular distance between L_1 and L_2, namely, the lane width. Fig. 1(b) depicts the side view of the camera and road geometry. The camera is installed at a height h above the ground plane and tilted (down) an angle ϕ. The direction of vector $\overrightarrow{CO}$ is perpendicular to the image plane. Point O is located on the ground plane and F is the length of vector $\overrightarrow{CO}$. The model is accurate if the road is flat and the rotation of the ground plane about the Z_C axis is negligible. Moreover, it has been pointed out that there is theoretically less than a 10% bias in distance measurements for road grades of 2% or less when using the reduced (two-angle) camera model [3]. Based on the pin-hole camera model, the perspective projection of a scene point in the camera's coordinate system onto the image coordinate frame can be described as

$$\begin{aligned} u &= -f\frac{X_C}{Z_C} \\ v &= -f\frac{Y_C}{Z_C} \end{aligned} \tag{1}$$

where f denotes the focal length.

As shown in Fig. 1(b), a point in the world coordinate system $O-XYZ$ is transformed into the camera's coordinate system $C - X_C Y_C Z_C$ by only a translation and a rotation. First, we rotate the world coordinate system an angle ϕ around the X axis to get the camera-shift coordinate system $O - UVW$

$$\begin{bmatrix} U \\ V \\ W \end{bmatrix} = \begin{bmatrix} 1 & 0 & 0 \\ 0 & \cos\phi & -\sin\phi \\ 0 & \sin\phi & \cos\phi \end{bmatrix} \begin{bmatrix} X \\ Y \\ Z \end{bmatrix} \tag{2}$$

Expression (2) can be further simplified because objects are assumed to lie on the ground plane where Z is equal to 0. Next, we shift the camera-shift coordinate frame from point O to point C along the vector $\overrightarrow{OC}$ and inverse V axis of the camera-shift coordinate frame to obtain the camera's coordinate system

$$\begin{bmatrix} X_C \\ Y_C \\ Z_C \end{bmatrix} = \begin{bmatrix} U \\ W \\ -V - F \end{bmatrix} = \begin{bmatrix} 1 & 0 \\ 0 & \sin\phi \\ 0 & -\cos\phi \end{bmatrix} \begin{bmatrix} X \\ Y \end{bmatrix} - \begin{bmatrix} 0 \\ 0 \\ F \end{bmatrix} \tag{3}$$

Applying (1) yields

$$\begin{aligned} u &= -f\frac{X_C}{Z_C} = -f\frac{X}{-Y\cos\phi - F} \\ v &= -f\frac{Y_C}{Z_C} = -f\frac{Y\sin\phi}{-Y\cos\phi - F} \end{aligned} \tag{4}$$

The image coordinate system is shown in Fig. 1(c) where the rectangular region represents the image display resulted from the image sensor. Solid line segments l_1 and l_2 represent a pair of parallel lane markings (L_1 and L_2 in Fig. 1(a)) that can be observed by the camera, and dashed lines represent the same lane markings which are out of the camera's view. The projections of the parallel lines in Fig. 1(a) will intersect at a vanishing point $VP(u_0, v_0)$ in the image coordinate frame. Assuming that the vanishing point lies at a position where $Y \to \infty$ and $X/Y = \tan\theta$ in world space, we can estimate u_0

and v_0 as

$$\begin{aligned} u_0 &= \lim_{Y\to\infty}\left(-f\frac{X}{-Y\cos\phi - F}\right) \\ &= \lim_{Y\to\infty}\left(-f\frac{Y\tan\theta}{-Y\cos\phi - F}\right) \\ &= f\tan\theta\sec\phi \end{aligned} \tag{5}$$

$$\begin{aligned} v_0 &= \lim_{Y\to\infty}\left(-f\frac{Y\sin\phi}{-Y\cos\phi - F}\right) \\ &= f\tan\phi \end{aligned} \tag{6}$$

Now consider some characteristic points on the lane markings l_1 and l_2 in the image (see Fig. 1(a) and (c)). We select p_1 and p_2 at the intersections of lines l_1 and l_2 with the u axis. The corresponding 3-D points P_1 and P_2 lie at the intersections of lines L_1 and L_2 with the X axis. Equation (4) shows the convenience of this selection, i.e., $Y = 0$ implies $v = 0$. The u-coordinates of p_1 and p_2 in the image can be expressed as

$$\begin{aligned} u_1 &= \frac{fX_1}{F} = \frac{f(X_2 - w\sec\theta)}{F} \\ u_2 &= \frac{fX_2}{F} \end{aligned} \tag{7}$$

Let $\Delta u = u_2 - u_1$ and given $F = h\csc\phi$, from (7) we obtain

$$\Delta u = \frac{fw\sec\theta}{F} = \frac{fw\sec\theta}{h\csc\phi} \tag{8}$$

These three expressions (5), (6), and (8) contain four unknowns: f, θ, ϕ, and h, so we have to add other *a prior* knowledge to resolve them.

III. Estimating the Camera Parameters

Based on the camera model and some useful expressions presented in Section II, in this section we estimate camera parameters, including f, θ, ϕ, and h. For other *a prior* knowledge, we consider two situations: 1) given the camera height, and 2) given the length of a land marking parallel to the road. Next, we will calibrate the traffic scene under these two situations.

A. Estimating the Camera Parameters Given the Camera Height

In many cases, the camera height can be easily measured using an ultrasonic device or other sensors. Given the camera height, we can recover the remaining parameters in virtue of expressions (5), (6), and (8). The computation process is described as follows.

According to (5), we have

$$\begin{aligned} {u_0}^2 &= f^2\tan^2\theta\sec^2\phi \\ &= f^2\tan^2\theta + f^2\tan^2\theta\tan^2\phi \end{aligned} \tag{9}$$

Using $v_0 = f\tan\phi$, (9) can be rewritten as

$$\begin{aligned} {u_0}^2 &= f^2\tan^2\theta + {v_0}^2\tan^2\theta \\ &= (f^2 + {v_0}^2)\tan^2\theta \\ &= (f^2 + {v_0}^2)(\sec^2\theta - 1) \end{aligned} \tag{10}$$

From (10), we obtain

$${u_0}^2 + f^2 + {v_0}^2 = (f^2 + {v_0}^2)\sec^2\theta \tag{11}$$

According to (6), we have

$$f^2 = {v_0}^2\cot^2\phi = {v_0}^2(\csc^2\phi - 1) \tag{12}$$

From (12), we obtain

$$f^2 + {v_0}^2 = {v_0}^2\csc^2\phi \tag{13}$$

Dividing (11) by (13), we have

$$\frac{{u_0}^2 + f^2 + {v_0}^2}{f^2 + {v_0}^2} = \frac{(f^2 + {v_0}^2)\sec^2\theta}{{v_0}^2\csc^2\phi} \tag{14}$$

From (8), we have

$$\csc\phi = \frac{fw}{h\Delta u}\sec\theta \tag{15}$$

Then (14) can be rewritten as

$$\frac{{u_0}^2 + f^2 + {v_0}^2}{f^2 + {v_0}^2} = \frac{(f^2 + {v_0}^2)\sec^2\theta}{{v_0}^2\left(\frac{fw}{h\Delta u}\right)^2\sec^2\theta} = \frac{f^2 + {v_0}^2}{\left(\frac{v_0 w}{h\Delta u}\right)^2 f^2} \tag{16}$$

Assuming $m = f^2$ and $B = \left(\frac{v_0 w}{h\Delta u}\right)^2$, then (16) becomes

$$\frac{m + {u_0}^2 + {v_0}^2}{m + {v_0}^2} = \frac{m + {v_0}^2}{Bm} \tag{17}$$

Rearranging (17), the focal length equation is obtained and expressed as:

$$am^2 + bm + c = 0 \tag{18}$$

where $a = B - 1$, $b = B{u_0}^2 + (B-2){v_0}^2$, and $c = -{v_0}^4$. The solution of (18) is m (or f^2) and it must be positive. Expression (18) is equivalent to the focal length equation in [9], but the computation process presented in this study is much more simplified, and the required parallel lane-marking lines are reduced to two ones from three ones.

After we get m from (18), the focal length is derived as

$$f = \sqrt{m} \tag{19}$$

From (6), the tilt angle is obtained as

$$\phi = \tan^{-1}\frac{v_0}{f} \tag{20}$$

From (5), the pan angle is obtained as

$$\theta = \tan^{-1}\frac{u_0}{f\sec\theta} \tag{21}$$

\phi

Because (18) is a binomial equation, its solutions must be further analyzed to determine the correct one in different cases. Since $c < 0$, it is easy to define that

1) For $a > 0$, the solution of m is

$$m = \frac{-b + \sqrt{b^2 - 4ac}}{2a} \tag{22}$$

2) For $a = 0$, there is only one analytical solution which is the correct solution.

3) For $a < 0$, there are two positive solutions; the correct solution is the one that satisfies the constraint of (8).

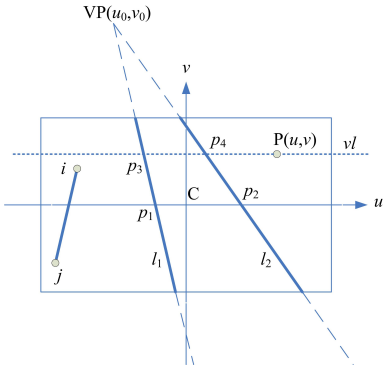

Fig. 2. Illustration of the virtual horizontal line *vl* and lane-marking lines in the image.

Next, we will discuss how camera parameters affect the sign of coefficient a. Analyzing a leads to

$$\begin{aligned} a = B - 1 &= \left(\frac{v_0 w}{h\Delta u}\right)^2 - 1 \\ &= \left(\frac{wf\tan\phi}{h\frac{fw\sec\theta}{h\csc\phi}}\right)^2 - 1 = \left(\frac{\cos\theta}{\cos\phi}\right)^2 - 1 \end{aligned} \tag{23}$$

Thus it is definite that
1) if $|\phi| > |\theta|$, then $a > 0$;
2) if $|\phi| = |\theta|$, then $a = 0$;
3) if $|\phi| < |\theta|$, then $a < 0$.

B. Estimating the Camera Parameters Given the Length of a Land Marking Parallel to the Road

Sometimes, it is not convenient or even possible to measure the camera height, but it is easy to attain the length of a land marking parallel to the road. Under this situation we must explore some other different strategy to resolve the equations of (5), (6), and (8). From (4), it can be confirmed that all points having the same Y coordinate in the world coordinate system will be projected onto a horizontal line in the image plane, i.e., Y and v are one-to-one corresponded. Moreover, if Y is fixed, u is positively proportional to X.

To construct the 3-D world coordinate $(X, Y, 0)$ of any point $P(u, v)$ in 2-D image space, we draw a virtual horizontal line through this point to intersect two lane markings l_1 and l_2 at p_3 and p_4 (see Fig. 2). The u-coordinates of p_3 and p_4 in the image are denoted as u_3 and u_4. Given $\Delta u = u_2 - u_1$ and let $\Delta u_{34} = u_4 - u_3$, the corresponding X coordinate of $P(u, v)$ can be easily inferred:

$$\begin{aligned} \frac{X}{u} &= \frac{w\sec\theta}{\Delta u_{34}} \\ \frac{\Delta u_{34}}{\Delta u} &= \frac{v - v_0}{0 - v_0} \end{aligned} \tag{24}$$

Solving for X, we obtain

$$X = \frac{v_0 w u\sec\theta}{\Delta u(v_0 - v)} \tag{25}$$

Assuming IJ is a land marking parallel to the road, the length of IJ in world space is known as d, and the perspective projection of IJ onto the image is ij (see Fig. 2), We can recover the pan angle of the camera as follows.

1) If $v_i > v_j$, we have

$$X_I - X_J = d\sin\theta \tag{26}$$

Substituting (25) into (26), we obtain

$$\frac{v_0 w u_i\sec\theta}{\Delta u(v_0 - v_i)} - \frac{v_0 w u_j\sec\theta}{\Delta u(v_0 - v_j)} = d\sin\theta \tag{27}$$

Rearranging (27), we obtain

$$\sin 2\theta = \frac{2v_0 w}{d\Delta u}\left(\frac{u_i}{v_0 - v_i} - \frac{u_j}{v_0 - v_j}\right) \tag{28}$$

2) Similarly, if $v_i < v_j$, we obtain

$$\sin 2\theta = \frac{2v_0 w}{d\Delta u}\left(\frac{u_j}{v_0 - v_j} - \frac{u_i}{v_0 - v_i}\right) \tag{29}$$

In typical situations we know beforehand that the pan angle of the camera lies in the range of $(-\frac{\pi}{4}, \frac{\pi}{4})$ to monitor wide areas of traffic scenes. Moreover, if $|u_0| < v_0$, dividing (5) by (6), we have

$$\frac{u_0}{v_0} = \frac{f\tan\theta\sec\phi}{f\tan\phi} \tag{30}$$

From (30), we get

$$|\tan\theta| = \left|\frac{u_0}{v_0}\right|\sin\phi < 1 \tag{31}$$

Thus, it is obvious that if $|u_0| < v_0$, then $\theta \in (-\frac{\pi}{4}, \frac{\pi}{4})$.

Now review (28) and (29), assuming $\sin 2\theta = T$, we get

$$\theta = \frac{1}{2}\sin^{-1} T \tag{32}$$

Solving for ϕ from (30), the tilt angle is obtained as

$$\phi = \sin^{-1}\frac{v_0\tan\theta}{u_0} \tag{33}$$

From (6), the focal length is obtained as

$$f = \frac{v_0}{\tan\phi} \tag{34}$$

From (8), the camera height is obtained as

$$h = \frac{fw\sec\theta}{\Delta u\csc\phi} \tag{35}$$

IV. Experimental Results

In this section we make some experiments on actual traffic scenes to demonstrate the proposed calibration method.

A. Recovery of Camera Parameters

The first experiment is the recovery of camera parameters using some lane markings painted on the road. Because the perspective projection of any set of parallel lines, which are not parallel to the image plane in world space, will converge to a vanishing point, we can utilize two lane-marking lines to estimate $VP(u_0, v_0)$ and Δu. Besides, either the camera height or the length of a lane marking parallel to the road is used to recover the camera parameters (Fig. 3).

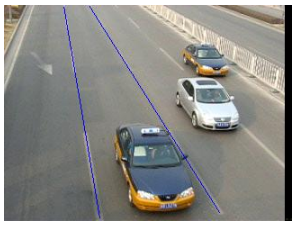

(a)

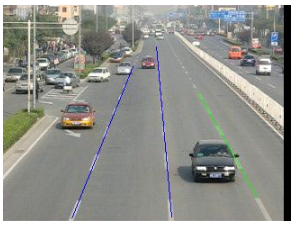

(b)

Fig. 3. Lane markings used for camera calibration.

(a)

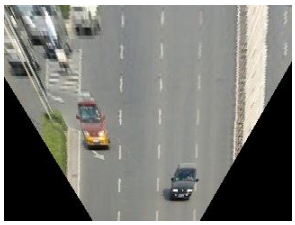

(b)

Fig. 4. Bird views of the images presented in Fig. 3.

TABLE I

PARAMETERS IN THE CAMERA CALIBRATION PROCESS

Parameter types	Calibrating the traffic Scene of Fig. 3(a)	Calibrating the traffic Scene of Fig. 3(b)
A prior knowledge	Two lane-marking lines with lane width: w = 3.35 m; Camera height: h = 6.88 m.	Two lane-marking lines with lane width: w = 3.35 m; A third lane-marking line with length: d = 60 m.
Intermediate variables	Vanishing point: $u_0 = -103.540$, $v_0 = 180.238$; $\Delta u = 86.1889$.	Vanishing point: $u_0 = 7.59903$, $v_0 = 110.345$; $\Delta u = 53.3378$.
Recovered camera parameters	Focal length: f = 548.333 pixels; Pan angle: $\theta = -0.178119$ rad; Tilt angle: $\phi = 0.318365$ rad.	Focal length: f = 1170.66 pixels; Pan angle: $\theta = 0.0065$ rad; Tilt angle: $\phi = 0.0940$ rad; Camera height: h = 6.9 m.

The camera height in the left traffic scene of Fig. 3 is known, while the length of a land marking line (represented as a green line) in the right traffic scene of Fig. 3 is known. We use the strategies presented in Section III to calibrate these two traffic scenes, and *a prior* knowledge, intermediate variables, and recovered camera parameters related to the calibrations are tabulated in Table I.

We also made quantitative comparisons between these two calibration strategies. In Fig. 3(a) where the camera height is known, we get the length of a land marking parallel to the road after camera calibration, then recalibrate the traffic scene using the second calibration strategy and get the same camera parameters. In Fig. 3(b) where the length of a land marking parallel to the road is known, we get the camera height after camera calibration, then recalibrate the traffic scene using the first calibration strategy and get the same camera parameters. These comparisons proved the proposed calibration method.

B. Inverse Perspective Transformation

After camera parameters have been recovered, we can reconstruct 3-D positions from the 2-D image. Naturally, (25) is used to obtain the X coordinate in world space. The computation of the Y coordinate is demonstrated as follows.

From (4), we have

$$\frac{u}{v} = \frac{X}{Y \sin\phi} \tag{36}$$

Substituting (25) into (36) and solving for Y, we get

$$Y = \frac{vX}{u \sin\phi} = \frac{v_0 wv}{\Delta u (v_0 - v) \sin\phi \cos\theta} \tag{37}$$

Fig. 4 depicts the inverse perspective images derived from the two camera images in Fig. 3.

C. Vehicle Dimension Measurement

In many visual traffic monitoring systems, vehicle class is an important traffic parameter. It is common sense that vehicle dimension is the most significant attribute to discriminate among different vehicle classes. With the aid of the deformable vehicle model [11], we measure 3-D vehicle dimension based on the proposed camera calibration method.

Vanishing point coordinates can be estimated from the camera parameters. We have obtained the vanishing point $VP(u_0, v_0)$ for lines parallel to the road. As any pair of parallel lines on the ground plane intersects at a point that lies on the vanishing line $v = v_0$ in the image coordinate frame, we can estimate the vanishing point (u_0', v_0') for lines perpendicular to the roadway as

$$\begin{aligned} u_0' &= -f \cot\theta \sec\phi \\ v_0' &= f \tan\phi \end{aligned} \tag{38}$$

From (1), (2), and (3), we obtain the vanishing point (u_0'', v_0'') for lines perpendicular to the ground plane as

$$\begin{aligned} u_0'' &= 0 \\ v_0'' &= -f \cot\phi \end{aligned} \tag{39}$$

By virtue of these three vanishing points, we manually set boundaries and place cuboids on hacks present in the video sequence (Fig. 5). We assume that the hacks are aligned with the road, and it can be seen that the cuboids fit hacks well in both video sequences. We further estimate the dimensions of twenty-three hacks and compare them with the actual values published by the manufacturers. The estimate values and their corresponding actual ones are shown in Fig. 6 and Table II.

In Table II, the most accurate estimation is on the hack width and the least accurate one is on the hack height. However, it can be seen from Fig. 5 that the hacks are not strictly cubic, for example, the bottom boundaries of the hack cuboids do not lie on the road surface and the top boundaries of the hacks are hollow, which caused the major errors for height estimation. We also fitted cuboids on

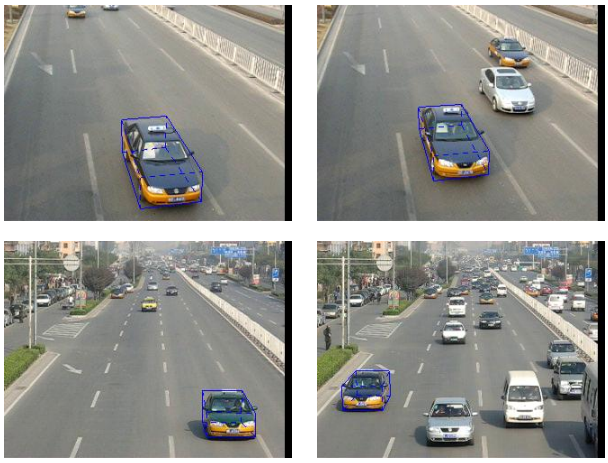

Fig. 5. Manually fitted cuboids on hacks using the calibration parameters.

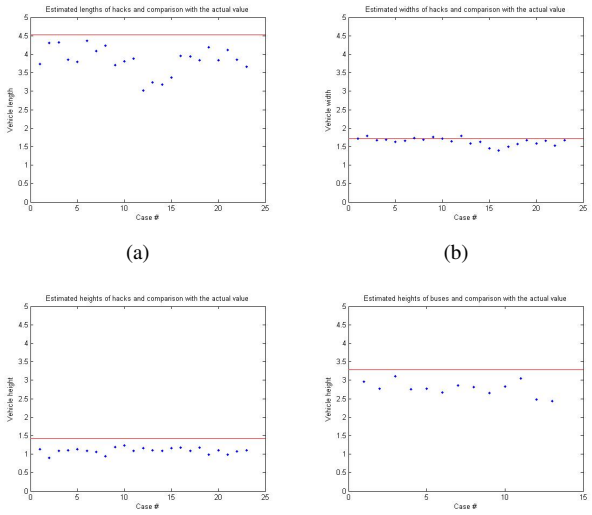

(a) (b)

(c) (d)

Fig. 6. Estimated dimensions of vehicles and comparisons with the actual values: (a) Estimated lengths of 23 hacks; (b) Estimated widths of 23 hacks; (c) Estimated heights of 23 hacks; (d) Estimated heights of 13 buses.

TABLE II

ESTIMATION ACCURACY OF THE VEHICLE DIMENSIONS

Vehicle dimensions	Estimate values	Actual values	Accuracy
Hack length	3.8390 m	4.525 m	84.8 %
Hack width	1.6414 m	1.725 m	95.1 %
Hack height	1.0941 m	1.425 m	76.8 %
Bus height	2.7797 m	$\approx$ 3.290 m	84.5 %

thirteen buses as shown in Fig. 7, estimated their heights, and made comparisons with the approximately actual value (see Fig. 6(d)). It is interesting that the estimation accuracy of bus height becomes 84.5% (see Table II). This can be attributed to the fact that buses are more cubic than hacks. If we take the deviation of 0.25 m $\pm$ 0.10 m into account when estimating the vehicle height as in [11], the average accuracy of dimension estimation can be further improved. Remaining errors come from three main factors: the first factor is the

Fig. 7. Manually fitted cuboids on buses.

camera calibration error; the second factor is that the vehicles are not strictly aligned with the roadway direction; and the third factor is that the cuboids do not perfectly fit the vehicles due to manual limitations.

V. CONCLUSION

In this paper we use easy attainable lane markings to calibrate traffic scenes. All required *a prior* knowledge contains two parallel lane-marking lines with known lane width, and either the camera height or the length of a lane-marking line parallel to the road. The proposed calibration method can be used to recover the focal length, the pan angle, the tilt angle, and even the camera height if necessary, and experiments proved its effectiveness. Two significant parameters related to the calibration approach are the vanishing point $VP(u_0, v_0)$ and Δu in the image coordinate frame, thus in future work we will pay attention to efficient automatic lane-marking recognition algorithms to improve the calibration accuracy and enhance the intelligence of VTMS.

REFERENCES

[1] B. Coifman, D. Beymer, P. McLauchlan, and J. Malik, "A real-time computer vision system for vehicle tracking and traffic surveillance," *Transportation Research Part C*, vol. 6, pp. 271-288, 1998.

[2] D. Koller, J. Weber, and J. Malik, "Robust multiple car tracking with occlusion reasoning," *in European Conference on Computer Vision*, 1994, pp. 189-196.

[3] T.N. Schoepflin and D.J. Dailey, "Dynamic camera calibration of roadside traffic management cameras for vehicle speed estimation," *IEEE Trans. Intell. Transport. Syst.*, vol. 4, no. 2, pp. 90-98, June 2005.

[4] R. Cucchiara, M. Piccardi, and P. Mello, "Image analysis and rule-based reasoning for a traffic monitoring system", *IEEE Trans. Intell. Transport. Syst.*, vol. 1, no. 2, pp. 119-130, June 2000.

[5] O. Masoud and N. Papanikolopoulos, "Using geometric primitives to calibrate traffic scenes," *in Proc. IEEE/RSJ Intl. Conf. Intelligent Robots and Systems*, vol. 2, 2004, pp. 1878-1883.

[6] P. Kummar, S. Ranganath, W. Huang, and K. Sengupta, "Framework for real-time behavior interpretation from traffic video," *IEEE Trans. Intell. Transport. Syst.*, vol. 6, no. 1, pp. 43-53, Mar. 2005.

[7] K. Mueller, A. Smolic, M. Droese, P. Voigt, and T. Wiegand, "Reconstruction of a dynamic environment with a fully calibrated background for traffic scenes," *IEEE Trans. Circuits and Systems for Video Technology*, vol. 15, no. 4, pp. 538-549, Apr. 2005.

[8] F.Y. Wang, "A simple and analytical procedure for calibrating extrinsic camera parameters," *IEEE Trans. Robotics and Automation*, vol. 20, no. 1, pp. 121-124, Feb. 2004.

[9] K.T. Song and J.C. Tai, "Dynamic calibration of Pan-Tilt-Zoom cameras for traffic monitoring," *IEEE Trans. Systems, Man and Cybernetics, Part B*, vol. 36, no. 5, pp. 1091-1103, Oct. 2006.

[10] Y.T. Li, Y.F. Ai, F.H. Zhu, and F.Y. Wang, "On automatic and dynamic camera calibration based traffic visual surveillance", *in Proc. IEEE Intelligent Vehicles Symposium*, June, 2007, pp. 358-363.

[11] A.H.S. Lai, G.S.K. Fung, and N.H.C. Yung, "Vehicle type classification from visual-based dimension estimation," *in Proc. IEEE Conf. Intell. Transport. Syst.*, Aug. 2001, pp. 201-206.